Structural characterization of copper(II) binding to α-synuclein: Insights into the bioinorganic chemistry of Parkinson's disease

Rodolfo M. Rasia*, Carlos W. Bertoncini*†, Derek Marsh‡, Wolfgang Hoyer*, Dmitry Cherny*, Markus Zweckstetter†, Christian Griesinger†, Thomas M. Jovin*, and Claudio O. Fernández*§¶

Departments of *Molecular Biology, ‡Spectroscopy, and †NMR-Based Structural Biology, Max Planck Institute for Biophysical Chemistry, Am Fassberg 11, 37077 Göttingen, Germany; and §Instituto de Biología Molecular y Celular de Rosario, Consejo Nacional de Investigaciones Científicas y Técnicas, Universidad Nacional de Rosario, Suipacha 531, S2002LRK, Rosario, Argentina

Edited by Harry B. Gray, California Institute of Technology, Pasadena, CA, and approved February 14, 2005 (received for review October 22, 2004)

The aggregation of α-synuclein (AS) is characteristic of Parkinson's disease and other neurodegenerative synucleinopathies. We demonstrate here that Cu(II) ions are effective in accelerating AS aggregation at physiologically relevant concentrations without altering the resultant fibrillar structures. By using numerous spectroscopic techniques (absorption, CD, EPR, and NMR), we have located the primary binding for Cu(II) to a specific site in the N terminus, involving His-50 as the anchoring residue and other nitrogen/oxygen donor atoms in a square planar or distorted tetragonal geometry. The carboxylate-rich C terminus, originally thought to drive copper binding, is able to coordinate a second Cu(II) equivalent, albeit with a 300-fold reduced affinity. The NMR analysis of AS–Cu(II) complexes reveals the existence of conformational restrictions in the native state of the protein. The metallobiology of Cu(II) in Parkinson's disease is discussed by a comparative analysis with other Cu(II)-binding proteins involved in neurodegenerative disorders.

amyloid | fibrillation | metallobiology

The protein α-synuclein (AS) is the main component of neuronal and glial cytoplasmic inclusions, pathologically described as Lewy bodies, that constitute the hallmark lesions of a group of neurodegenerative diseases collectively referred to as synucleinopathies (1, 2). The identification of point mutations and locus triplication in the AS gene as sole causes of familial inherited Parkinson's disease (PD) (3, 4) has stimulated research on the mechanism of AS neurotoxicity.

AS comprises 140 amino acids distributed in three different regions: (*i*) the amphipathic N terminus (residues 1–60); (*ii*) the highly hydrophobic self-aggregating sequence known as NAC (non-Aβ component, residues 61–95), which is presumed to initiate fibrillation (5); and (*iii*) the acidic C-terminal region (residues 96–140). In its native monomeric state, AS adopts an ensemble of conformations with no significant secondary structure (6, 7), although long-range interactions have been shown to stabilize an aggregation-autoinhibited global protein architecture (8, 9). The protein undergoes dramatic conformational transitions from its natively unstructured state to an α-helical conformation upon interaction with lipid membranes (10, 11) or to the characteristic crossed β-conformation in highly organized amyloid-like fibrils under conditions that trigger aggregation (12, 13). Whereas the mechanism for the α-helical transition is well understood, the detailed mechanism of amyloid formation remains to be elucidated.

The kinetics of fibrillation of AS are consistent with a nucleation-dependent mechanism (14), being modulated by factors and effectors of different types. Among them, low pH and high temperature (15–17), organic solvents (18), heparin (19), polyamines (14, 20), and metal cations (21–23) accelerate AS aggregation. Not only do metal cations exert a physiological influence on protein structure, but transition metals have been also frequently recognized as risk factors in neurodegenerative disorders (24, 25). Brain lesions associated with Alzheimer's disease (AD) are rich in Fe(III), Zn(II), and Cu(II) (26). Recent biophysical and structural studies of the amyloid precursor protein and the amyloid-β peptide (Aβ) have provided strong evidence linking Cu(II) with AD (27–31). Furthermore, a role for copper in prion disease has also been suggested, and the interaction of Cu(II) with fragments of the prion protein was structurally characterized (31–34).

Although less well defined, the metallobiology of PD is attracting increasing attention. Iron deposits have been identified in Lewy bodies in the substantia nigra (35) and elevated Cu(II) concentrations have been reported in the cerebrospinal fluid of PD patients (36). Based on this evidence, a role was suggested for copper and iron in the catalysis of oxidative oligomerization and subsequent aggregation of AS in the presence of hydrogen peroxide (37, 38). A systematic analysis of the effect of various metal ions revealed that Al(III), Fe(III), and Cu(II) accelerate AS fibrillation *in vitro* (22), and another study showed that Cu(II) is the most effective ion in promoting AS oligomerization (21). The enhancement of fibrillation by metals has been attributed to Coulombic screening of charge–charge repulsion associated with the highly acidic C-terminal domain (21, 22).

The reported effects of transition metal ions on AS fibrillation were examined at concentrations (0.5–5.0 mM) far greater than those normally occurring in tissues (21–24), such that the physiological relevance of these effects is open to question. Furthermore, neither the structural characterization of the binding sites nor the identification of the amino acids involved in the interaction has been carried out. Performing experiments under more physiologically relevant conditions by using high-resolution spectroscopic techniques would serve to establish the role of metal ions in synucleinopathies at the molecular resolution currently available for other amyloidoses. One could then address the central question of whether these agents constitute a common denominator underlying the amyloid-related disorders known as AD, PD, and prion disease.

The present work focuses on the interactions of Cu(II) and AS at single-residue resolution. We demonstrate that substantially lower levels of Cu(II) than those used in previous studies are sufficient for accelerating AS aggregation. Using a combination of low- and high-resolution spectroscopic techniques, we identified and characterized two distinct Cu(II)-binding motifs in AS. A high-affinity copper-binding site encompassing a complex

This paper was submitted directly (Track II) to the PNAS office.

Abbreviations: AS, α-synuclein; PD, Parkinson's disease; AD, Alzheimer's disease; DEPC, diethylpyrocarbonate; Aβ, amyloid β peptide; NAC, non-Aβ component.

¶To whom correspondence should be addressed. E-mail: cfernan@gwdg.de.

conformational array is located in the N terminus of the protein. The structural and biological implications of copper binding to AS, as well as its role in PD, have to be reconsidered based on these findings and are discussed in this paper.

Experimental Procedures

Protein Preparation and Purification. Unlabeled and ^{15}N-labeled wild-type and truncated (1–108) AS was prepared as described (14). The C-terminal AS peptide (95–137) was synthesized with an Applied Biosystems 433A synthesizer and standard solid-phase Fmoc chemistry.

The sole His-50 residue was blocked by reaction with diethylpyrocarbonate (DEPC) (39). The modification yield was >95%.

Aggregation Assays. AS aggregation measurements were performed in triplicate on 100 μM AS samples dissolved in buffer A (20 mM Mes-Na/100 mM NaCl, pH 6.5). Samples were incubated with 0, 40, 100, and 200 μM $CuSO_4$ at 37°C in glass vials under constant stirring (300 rpm). The degree of aggregation was estimated from aliquots (5 μl) taken at different time points by using the Thioflavin-T fluorescence assay (16, 40).

Aggregation yields were normalized to the final values and the averaged data points fitted to the kinetic model used previously (14), $\alpha[t] = (1 - e^{-k_{app}t})/(1 + e^{-k_{app}(t-t_{1/2})})$, in which k_{app} is the apparent aggregation rate constant, and $t_{1/2}$ is the lag time to the midpoint of the fractional transition from monomer to aggregate, $\alpha[t]$, measured by the Thioflavin-T assay.

Electron Microscopy. An aliquot was removed from the aggregation incubation mixture and adsorbed onto a carbon film as described (16). The samples were analyzed with a Philips (Eindhoven, The Netherlands) CM12 electron microscope operated in an angular dark-field mode.

Cu(II) Content Determination. The salt used for Cu(II) solutions was $CuSO_4$. Cu(II) concentrations were measured by using 4-(2-pyridylazo)resorcinol (41). The calibration yielded the relationship $[Cu(II)](\mu M) = (27.1 \pm 0.3)\cdot\Delta A_{504\ nm} + (0.1 \pm 0.1)$.

Equilibrium dialysis was used to determine the binding of Cu(II) to monomeric AS at different Cu(II) concentrations. Five hundred microliters of a 50-μM metal-free AS solution in buffer A was dialyzed for 36 h against 500 ml of the same buffer containing 0, 1, or 10 μM $CuSO_4$. The buffer solution was changed every 12 h.

To estimate [Cu(II)] in AS aggregates, 150 μl of the aggregation assay was withdrawn and centrifuged at 90,000 $\times$ *g*. The pellets were separated from supernatants and redissolved in 150 μl of 5.75 M guanidine HCl. Cu(II) concentrations were then measured in both fractions (supernatants and redissolved pellets).

Absorption and CD Spectroscopy. Visible electronic absorption spectra were obtained on a Varian Cary 100 Scan spectrophotometer. CD spectra were acquired with a Jasco (Gross-Umstadt, Germany) 720 spectrapolarimeter. Cu(II) titration experiments were performed at 15°C on samples containing 300 μM protein in buffer A. Aggregation did not occur under these conditions of low temperature and absence of stirring. Data were expressed as difference absorbance (E) or CD (ΔE) per molar concentration of protein. Spectrophotometric data were fit by using the program DYNAFIT (42).

EPR Spectroscopy. EPR spectra were recorded on a Varian Century-Line 9-GHz spectrometer. Samples containing 300 μM protein in buffer A were placed in a standard quartz EPR tube and immersed in a liquid-nitrogen dewar. The static magnetic field was measured with a Bruker (Rheinstetten, Germany) ER 035M NMR magnetometer and the microwave frequency with a Hewlett–Packard 5345A/5355A frequency counter.

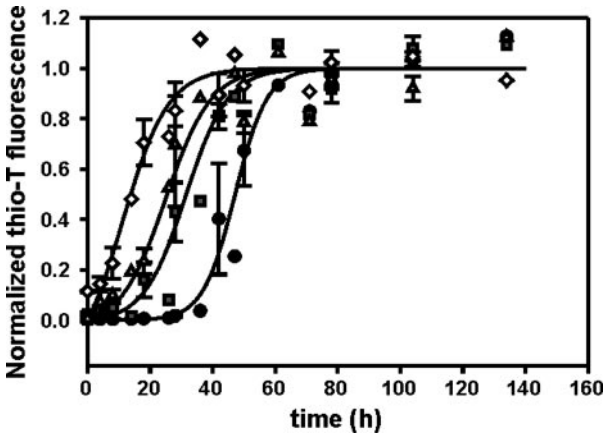

Fig. 1. Aggregation kinetics of 100 μM AS in the presence of 0 (●), 40 (■), 100 (▲), and 200 (◇) μM Cu(II). Error bars correspond to standard deviations of three independent experiments. Solid lines represent fits according to the model given in the text. The fits yielded the following parameters: k_{app} (h^{-1}) = 0.19 ± 0.03, 0.15 ± 0.05, 0.14 ± 0.05, 0.14 ± 0.01, and $t_{1/2}$ (h) = 47 ± 5, 31 ± 4, 25 ± 3, 11 ± 3 [in order of increasing Cu(II) concentration].

NMR Spectroscopy. NMR spectra were acquired on a Bruker DRX 600 NMR spectrometer by using a triple-resonance probe equipped with *z* axis self-shielded gradient coils. All NMR experiments were performed with pulsed-field gradient enhanced pulse sequences on a 100-μM sample of AS in buffer A at 15°C.

^{1}H-^{15}N heteronuclear single quantum correlation (HSQC) amide crosspeaks affected during Cu(II) titration were identified by comparing their intensities (*I*) with those of the same crosspeaks (I_0) in the data set of samples lacking Cu(II). The I/I_0 ratios of 95–105 nonoverlapping crosspeaks were plotted as a function of the protein sequence to obtain intensity profiles. Acquisition, processing, and visualization of the spectra were performed as described (14).

Results

Cu(II) Levels in the Micromolar Range Are Effective in Inducing AS Aggregation. The time course of AS aggregation was monitored at 37°C by the standard Thioflavin-T fluorescence assay (16, 40). Addition of 40–200 μM Cu(II) decreases the characteristic lag time for aggregation of the unliganded protein to a degree that depends on Cu(II) concentration (Fig. 1). An inverse relationship was found between $t_{1/2}$ and Cu(II) concentration, but no major changes were observed in the rate of aggregate growth (k_{app}).

Seventy percent to 90% of the Cu(II) used in the aggregation assay was incorporated into the AS aggregates. A morphological analysis by electron microscopy of the aggregates formed upon incubation with 40–200 μM Cu(II) revealed fibrillar structures qualitatively similar to those obtained in the absence of the metal ion (Fig. 5 *A* and *B*, which is published as supporting information on the PNAS web site).

Cu(II) Binding to AS Monitored by Absorption and CD Reveals the Presence of Different Binding Sites. Initial estimates of the dissociation constant for Cu(II) binding to AS were provided by equilibrium dialysis. Cu(II)/protein ratios of 0.9 and 1.4 were determined after dialysis of a metal-free AS solution against buffer containing 1 or 10 μM Cu(II), respectively. Thus, AS is able to bind more than one equivalent of Cu(II) with dissociation

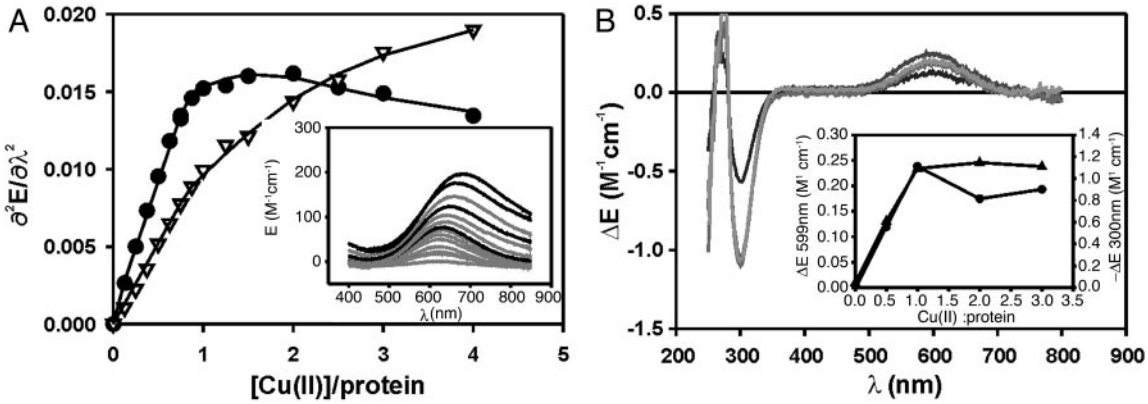

Fig. 2. Absorption and CD spectroscopy of Cu(II)–AS complexes. (*A*) Direct titration of AS with Cu(II). Concentration dependence of the second derivative absorbance at 620 (●) and 660 (▽) nm. Solid lines show the result of the simultaneous fit of both sets of data points as described in the text. (*Inset*) Ligand field region of the spectra. Black lines highlight the spectra at 1, 2, 3, and 4 equivalents of Cu(II). (*B*) CD spectra of wild-type AS. Spectra correspond to (from black to light gray) 0.5, 1, 2, and 3 equivalents of Cu(II) added to the protein. (*Inset*) ΔE values at 300 nm (▲) and at 599 nm (●) vs. Cu(II) concentration.

constants <1 and >10 μM. When a solution of AS containing one equivalent of Cu(II) was dialyzed against a metal-free buffer, a Cu(II)/protein ratio of 0.26 was obtained, demonstrating both the reversibility and high affinity of the Cu(II)–AS complexes.

Cu(II) binding was monitored by visible electronic absorption and CD spectroscopy upon titrations of AS with increasing concentrations of added Cu(II). At substoichiometric Cu(II)/AS ratios, a single visible absorption band appeared in the electronic spectra at ≈620 nm, saturating at one equivalent with $\varepsilon = 70$ $M^{-1}\cdot cm^{-1}$, typical of a Cu(II) d-d transition (Fig. 2*A Inset*). The absorption maximum (λ_{max}) is sensitive to the identity of the metal ligands and can be used as an indication of the number of nitrogen ligands bound to the Cu(II) ion (43). The visible absorption spectrum of the Cu(II)–AS complex was characteristic of two- or three-nitrogen coordination in a type (II) square-planar or distorted tetragonal arrangement. Beyond one equivalent of Cu(II), the visible absorption band increased in intensity and shifted toward lower energy. Subtraction of the spectrum recorded with one equivalent of Cu(II) revealed an absorption band with a maximum at 720 nm, likely reflecting the incorporation of a second Cu(II) ion into a different coordination environment. Analysis of the second derivatives ($\partial^2E/\partial\lambda^2$) of the spectra yielded quantitative information. The plot of this quantity at 620 nm showed discontinuities in the binding curve at one and two molar equivalents of Cu(II) (Fig. 2*A*). However, the absorbance curves recorded up to four equivalents of Cu(II) did not saturate. Thus, we fit the data according to a model incorporating complexes of Cu(II) in three classes of independent noninteractive binding sites per AS molecule: (*i*) a high-affinity site (K_{d1}); (*ii*) a lower-affinity site (K_{d2}); and (*iii*) a class of nonspecific n sites with very low affinity (K_{d3}/n).

The molar derivative absorbance signal [$(\partial^2E/\partial\lambda^2)$] corresponding to the above scheme is given by

$$\Delta\left(\frac{\partial^2 E}{\partial\lambda^2}\right) = \sum_{k=1}^{3} \alpha_k\delta_k\,, \qquad [1]$$

where α_k and δ_k are the relative fractional concentration and the molar difference absorbance second derivative, respectively, associated with formation of the Cu(II) complex(es) at site k. Analysis according to these models yielded the following dissociation constants: $K_{d1} = 120 \pm 160$ nM, $K_{d2} = 36 \pm 36$ μM, and $K_{d3}/n = 470 \pm 80$ μM. Despite the large numerical uncertainties associated with these quantities, due to the high concentration of protein required to achieve accurately measurable signals ($[AS]_{tot} \gg K_{d1,2}$), their relative order of magnitude was well established.

The CD spectra of AS complexed with Cu(II) showed a positive band in the d-d region (≈600 nm) and a negative band at 300 nm (Fig. 2*B*). The latter can be assigned to a charge transfer transition (c.t.) between the metal center and an imidazole group (π_1 $N_{im}-Cu$ c.t., 280–345 nm) or a deprotonated peptide nitrogen (^-N-Cu c.t., 295–315 nm) (44). The CD band at 300 nm saturated with one equivalent of added Cu(II) (Fig. 2*B Inset*). In contrast, the intensity of the CD band at 600 nm increased up to one equivalent of Cu(II), decreased upon further addition up to two equivalents of Cu(II), and remained constant at higher Cu(II) concentrations. We conclude that the c.t. band is associated with the highest-affinity Cu(II)-binding site. The decrease in ellipticity at 600 nm observed with more than one equivalent of Cu(II) probably reflects the development of a negative band associated with formation of the second Cu(II) complex.

Cu(II) Binding to AS Truncation Mutants. The contributions of different regions of the protein to Cu(II) binding were evaluated by following the association of Cu(II) with AS 1–108 (C-terminal truncated) and AS 95–137 (N-terminal truncated) peptides. Spectrophotometric titrations showed that both species bind Cu(II). Although the absorption spectrum of the Cu(II)–AS 1–108 complex was similar to that of the wild-type protein, the ligand field absorption band in the spectra of AS 95–137 was considerably red-shifted (data not shown). These results suggest that the high-affinity Cu(II)-binding site is located at the N terminus. The CD spectra of both truncated species displayed even stronger differences. The Cu(II)–AS 1–108 complex closely matched that of the full-length AS, from which we conclude that the geometry and position of the ligand set observed in the whole protein are highly conserved in the AS 1–108 fragment (Fig. 6*A*, which is published as supporting information on the PNAS web site). Conversely, the truncated form 95–137 showed an intense negative band in the visible region at ≈700 nm ($\Delta\varepsilon_{700} = -0.5$ $M^{-1}\cdot cm^{-1}$) and a positive band centered at 324 nm, assigned to a ^-N-Cu c.t. band (Fig. 6*B*). These results establish the contribution of the N-terminal fragment to the CD spectra of the Cu(II) complex of the whole protein; the Cu(II) complex of the C-terminal fragment is not able by itself to recreate any of the Cu(II)-binding sites of AS.

Mapping the Cu(II)-Binding Interfaces in AS by NMR. We explored the details of Cu(II) binding to AS by NMR spectroscopy. ^1H-^{15}N

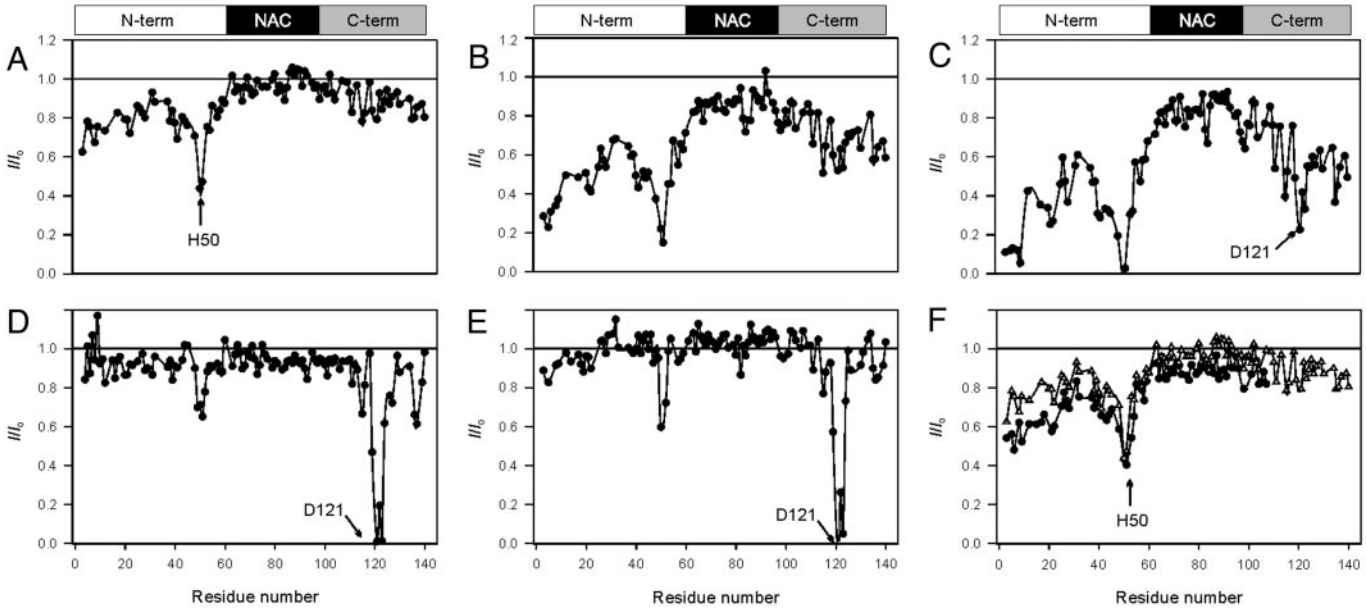

Fig. 3. I/I_0 profiles of the ^1H-^{15}N heteronuclear single quantum correlation NMR signals of 100 μM AS at pH 6.5 (except in *E*). (*A*) Concentration: 20 μM Cu(II). (*B*) Concentration: 40 μM Cu(II). (*C*) Concentration: 60 μM Cu(II). (*D*) DEPC-modified AS, 20 μM Cu(II). (*E*) Concentration: 20 μM Cu(II), pH 5.0. (*F*) Wild-type (Δ) and 1–108 (●) AS, 20 μM Cu(II).

heteronuclear single quantum correlation spectra contain one crosspeak for each amide group in the molecule (except those involving prolines) and thus provide multiple probes for locating the Cu(II)-binding sites. The electron spin relaxation from the paramagnetic Cu(II) results in the differential broadening (lower intensities) of the amide resonances linked to the paramagnetic center by through-bond or through-space interactions, providing the means for mapping the metal-binding interfaces in the protein.

We first recorded a series of ^1H-^{15}N heteronuclear single quantum correlation spectra of 100 μM AS at pH 6.5 in the presence of increasing concentrations of Cu(II) (0–60 μM) (Fig. 3 *A–C*). Significant changes in crosspeak intensities occurred in well defined regions of AS. The strongest broadening effects at 20 μM Cu(II) were centered on the amide group of His-50 in the N-terminal region, whereas little or no broadening was observed for the amide groups of residues located in the NAC region or belonging to the C-terminal domain. Thus, the N-terminal region was the most affected by Cu(II) binding under this condition. The broadening was further pronounced at 40–60 μM Cu(II), as reflected in values of $I/I_0 < 0.2$ for the resonances corresponding to residues 3–9 and 49–52. Residues 15–45 were also involved, but to a lesser extent. In addition, the I/I_0 profile of the C-terminal region revealed significant changes in the region comprising residues 110–140, the strongest effects being centered on Asp-121. Interestingly, the amide resonances assigned to the NAC region remained unaltered at the higher Cu(II) concentrations. All NMR spectral changes induced by Cu(II) were abolished upon EDTA addition, confirming the reversibility of Cu(II) binding.

The Cu(II) titration monitored by NMR showed that the residues encompassing His-50 were the most perturbed, suggesting that the imidazole ring plays a critical role in anchoring the Cu(II) ion to the N-terminal domain. Thus, we tested whether modification of histidine with DEPC affects the Cu(II)-binding features of AS. Exposure to DEPC shifted the paramagnetic influence of Cu(II) from the N- to the C-terminal domain (Fig. 3*D*), manifested by substantial changes in crosspeak intensities at Cu(II) concentrations as low as 20 μM. The strongest effects were centered on the amide group of Asp-121, whereas resonances in the NAC domain remained unaffected under these conditions. The decrease in intensity of the signals corresponding to residues 49–52 was likely due to residual Cu(II) coordination capability of His-50, e.g., through the imidazole N atom unmodified by DEPC. In summary, Cu(II) binding to DEPC-treated AS clearly shows the existence of two different copper-binding interfaces in the protein.

Because protonation of His-50 should reduce Cu(II) binding, we determined the pH dependence of Cu(II) binding to AS in the range of 5.0–6.5 (Fig. 7, which is published as supporting information on the PNAS web site). The I/I_0 profile measured at pH 5.0 and 20 μM Cu(II) is shown in Fig. 3*E*. The strongest broadening effects corresponded to the C-terminal domain, again centered on Asp-121, with a smaller effect evident in the N-terminal domain, located at His-50. The crosspeaks of residues in the NAC region remained insensitive to Cu(II) at pH 5.0.

It is worth noting that even when the most affected crosspeaks in the N-terminal region were severely broadened under conditions favoring Cu(II) binding (pH 6.5), signals were still detected at 40–60 μM Cu(II) (Fig. 3 *B* and *C*). In contrast, upon DEPC modification or protonation of His-50, Cu(II) concentrations as low as 20 μM were sufficient to broaden beyond detection the resonances of the most affected residues in the C-terminal region (Fig. 3 *D* and *E*). This behavior presumably reflects differences in the exchange dynamics and residence times of the two Cu(II)-binding sites in AS and supports the assignment of the N-terminal region as the high-affinity interface.

The interaction of the C-terminal truncated species AS 1–108 with Cu(II) was studied with the aim of understanding further the structural contribution of the C terminus to the overall binding process. The I/I_0 profiles in the Cu(II) concentration range of 0–60 μM at pH 6.5 were almost identical to those obtained with wild-type AS (Fig. 3*F*), confirming that the binding of Cu(II) to the N-terminal region of AS is independent of the presence of the C terminus.

The chemical shifts of all resonances were essentially unaltered upon Cu(II) binding to AS under the different conditions,

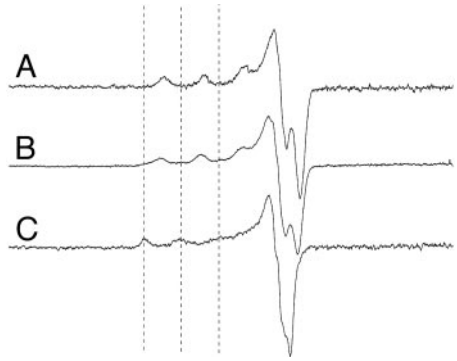

Fig. 4. EPR spectra (9 GHz) of Cu(II) bound to AS (1:1 molar ratio). (*A*) pH 6.5. (*B*) pH 5.0. (*C*) DEPC-modified at pH 6.5; T = 77 K, center field = 0.297 T; scan width = 0.2 T; ν = 9.146 GHz. Dotted vertical lines correspond to the three lower hyperfine lines in the DEPC-modified sample.

with the notable exception of the crosspeak assigned to Asp-119 ($|\Delta\delta\ ^{15}N| \geq 0.9$ ppm).

Cu(II) Coordination in the Complex with AS Studied by EPR. The 9-GHz EPR spectra of AS-Cu(II) and DEPC-modified AS–Cu(II) complexes (Fig. 4) were characteristic of Type 2 Cu(II) proteins (45). The Cu(II) complexes with the modified and unmodified protein at pH 6.5 differed qualitatively, in that the spectrum of the former extended to a significantly lower field and lacked an overshoot line in the $g\perp$ region. The Cu(II) hyperfine splittings and *g* values in the low-field parallel region were $A_{//} = 186$ and $176 \times 10^{-4}\cdot cm^{-1}$ and $g_{//} = 2.223$ and 2.316 ($g\perp \approx 2.05$ and 2.06) for the unmodified and modified protein, respectively. The Cu(II) EPR spectrum of the unmodified protein at pH 5.0 (Fig. 4*B*) resembled that of the unmodified protein at pH 6.5 but also clearly contained a weaker spectral component corresponding to the DEPC-modified protein (Fig. 4*C*). The appearance of the latter lower-affinity component agrees fully with the NMR results at pH 5.0.

Fig. 8, which is published as supporting information on the PNAS web site, provides a plot of $A_{//}$ vs. $g_{//}$ for various small-molecule Cu(II) complexes by using data from the literature that show the dependence of these parameters on the type of ligands in the complexes (46, 47). The EPR data from Cu(II) bound to unmodified AS at pH 6.5 correlated rather well with those for Cu(II) complexes with two nitrogen and two oxygen ligands (N_2O_2), whereas in the case of AS with modified histidine, the EPR parameters were indicative of four oxygen ligands (O_4).

Discussion

The neurobiology of metal ions has attracted growing interest by virtue of their link to major neurological syndromes. In this study, we found that Cu(II) levels substantially lower than those used previously (21, 22) are effective in accelerating the aggregation of AS. Cu(II) promotes nucleation but not the growth phase, suggesting that the Cu(II)-bound form of AS is more prone to nucleate than the unliganded protein, a feature observed previously for polyamine complexes (14). The presence of Cu(II) in the fibrils indicates that the protein aggregates in its copper-bound form. Interestingly, Cu(II) does not affect the structural features inherent to the spontaneous aggregation of AS, inasmuch as copper-induced fibrils exhibit the same morphology as those formed in the absence of the cation.

Previous studies suggested that AS was able to bind five or more copper ions with a K_d of 45–60 μM (21, 48). We show here that the protein tightly binds only two Cu(II) ions per monomer with dissociation constants in the 0.1- to 50-μM range. More Cu(II) ions can be ligated by the protein, but with significantly lower affinity and probably via nonspecific electrostatic interactions with charged amino acid side groups.

We find that at substoichiometric levels, Cu(II) mainly interacts with residues located in the N-terminal region of AS. This result is unexpected, because Cu(II) was previously claimed to bind exclusively to the negatively charged C-terminal region (21, 22). Different clusters of residues at the N terminus are clearly affected by Cu(II) binding, with amino acids 3–9 and 49–52 showing the strongest effect, whereas amino acids 20–24 and 39–44 were less affected. The broadening effect of a type II Cu(II) site on the amide resonances reaches ≈11 Å from the Cu(II) location (49). Thus, a decrease in intensity of a resonance does not necessarily indicate the direct participation of the corresponding residue in the coordination of the metal ion. Nevertheless, upon modification of His-50 by DEPC, the entire N-terminal region loses the ability to interact with the metal, demonstrating the role of this residue as the anchor for Cu(II) binding and indicating the involvement of the affected regions in the formation of a single Cu(II)-binding interface. In fact, modification of His-50 causes measurable changes in the chemical shifts of residues 49–52 and 3–9 (Fig. 9, which is published as supporting information on the PNAS web site), implying that both regions are in spatial proximity, most likely delineating a long-range preformed topology in the N-terminal region of the protein. This finding also correlates with the Cu(II) coordination environment described by EPR, characterized by two N and two O ligand atoms. His-50 provides one nitrogen ligand, implying that the source of the other nitrogen comes either from the amide backbone or the N-terminal NH_2 group. The oxygen ligands could be provided by water molecules or/and backbone carbonyls from the peptide.

A second lower-affinity binding motif for Cu(II) in AS is located at the C terminus. The affected region comprises residues 110–140, which also constitute the primary binding site for the polycationic polyamines (14). However, as demonstrated upon DEPC modification or protonation of the His-50, Cu(II)–AS interaction within this interface is initially highly localized around residues 119–123, the spectral features of which are most affected. Thus, we conclude that Asp-119, Asp-121, Asn-122, and Glu-123 likely represent the ligand set for the second metal ion. Correspondingly, EPR spectroscopy indicates that the Cu(II) atom bound to DEPC-modified AS has four oxygen donors, suggesting the involvement of carboxylates as major contributors to metal binding.

Several structural features of the native state of AS are implied by this study. Formation of a single metal-binding interface in the N-terminal region, involving residues widely separated in the primary amino acid sequence, implies that this domain folds back on itself and suggests that the protein must adopt a narrow set of conformations in solution rather than a fully random structure. The broadening profile induced by Cu(II) delimits the NAC region and strongly supports our hypothesis that a common feature of the ensemble of conformations adopted by AS in solution is the isolation of the NAC domain from the surrounding environment (8, 9, 14).

The absence of significant conformational changes of AS upon Cu(II) binding, shown by the invariance of the chemical shifts of the backbone amide groups and of the far-UV CD spectra (8), raises the question of what constitutes the basis for the enhancement of aggregation. We recently proposed (9, 14) that polyamine-induced AS aggregation is triggered by release of long-range interactions and residual structure in the C-terminal region, which otherwise protect the amyloidogenic NAC region from being exposed to solvent. An appealing hypothesis is that Cu(II) binding perturbs N-terminal long-range interactions that are critical for stabilizing a soluble native-like but autoinhibited conformation of AS. The most evident target for these interac-

Table 1. Structural and binding properties of high-affinity Cu(II) sites in amyloidogenic proteins involved in AD, prion disease, and PD

	AD		Prion disease	PD
Protein/peptide	APP	Aβ*	PrP†	AS
Ligand donor set	2N1O1S	3N1O	3N1O/2N2O	2N2O
Coordination‡	T	DT	S/DT	S/DT
Anchoring residue	His	His	His	His
K_d, μM	≈0.01	0.3–4	0.1–10	≈0.1
Stoichiometry	1:1	1:1	1:1	1:1
References	27, 51	29, 30, 52, 53	32–34, 54, 55	This work

APP, amyloid precursor protein; PrP, prion protein.

*Aβ_{1-40}, Aβ_{1-42}.

†Reported data correspond to the octarepeat-binding motif.

‡Coordination geometry: T, tetrahedral; S, square-planar; DT, distorted tetragonal.

tions is the imidazole moiety of His-50, which most probably coordinates Cu(II) directly.

That Cu(II) can promote AS aggregation efficiently at physiologically relevant concentrations and the identification of a binding interface in the N terminus for which Cu(II) has the highest affinity constitute important findings of this work and support the notion of PD as a metal-associated neurodegenerative disorder. At this juncture, a tighter link with other amyloid-related disorders such as AD and prion disease can be sought, based on the insights into the structural basis of copper interactions with AS gained in the present study. The key factors of AD and prion diseases are the amyloid precursor protein (APP) and prion protein (PrP), respectively. As shown in Table 1, the principal feature of Cu(II) binding to APP, PrP, and AS is the presence of His residues acting as anchoring sites and allowing coordination with other nitrogen, oxygen, or sulfur donors in 2N1O1S, 2N2O, or 3N1O arrangements. In all cases, the proteins bind one copper atom per site. Interestingly, the affinity of Cu(II) for these proteins is in the low or submicromolar range, a fact that may have important biological implications. Even if the intracellular Cu(II) pools are regulated by binding to ligands (i.e., metallothioneins) of various affinities, the coordination of Cu(II) by these ligands is labile and subject to fluctuation. We propose that the concentrations of Cu(II) in neurons and glia are sufficient to contribute to potential abnormal interaction with proteins such as AS under certain adverse circumstances. Furthermore, although the metabolic pathways of extracellular Cu(II) are poorly understood, Cu(II) levels as high as 15 μM can be envisioned (50), sufficient to form complexes with extracellular targets implicated in diseases such as Aβ. Although more studies are needed to explore other biological aspects of Cu(II)–AS interactions, the structural features emerging from this work indicate that perturbations in copper metabolism may constitute a more widespread element in neurodegenerative disorders than has been recognized previously.

We thank Mrs. B. Angerstein for recording the EPR spectra. C.O.F. thanks Fundación Antorchas and Agencia Nacional de Promoción Científica y Tecnológica (ANPCyT) for financial support. This work was supported by the Max Planck Society, the Fonds der Chemischen Industrie, and the Deutsche Forschungsgemeinschaft (DFG). It was within the scientific scope of the DFG Center for Molecular Physiology of the Brain (CMPB) in Göttingen as well as Graduiertenkolleg GRK 782. C.O.F. and R.M.R. are recipients of fellowships from the Alexander von Humboldt Foundation. M.Z. is the recipient of a DFG Emmy Noether Fellowship (ZW 71/1-4).

1. Goedert, M. (2001) *Nat. Rev. Neurosci.* **2,** 492–501.
2. Spillantini, M. G., Schmidt, M. L., Lee, V. M., Trojanowski, J. Q., Jakes, R. & Goedert, M. (1997) *Nature* **388,** 839–840.
3. Polymeropoulos, M. H., Lavedan, C., Leroy, E., Ide, S. E., Dehejia, A., Dutra, A., Pike, B., Root, H., Rubenstein, J., Boyer, R., *et al.* (1997) *Science* **276,** 2045–2047.
4. Singleton, A. B., Farrer, M., Johnson, J., Singleton, A., Hague, S., Kachergus, J., Hulihan, M., Peuralinna, T., Dutra, A., Nussbaum, R., *et al.* (2003) *Science* **302,** 841.
5. Giasson, B. I., Murray, I. V., Trojanowski, J. Q. & Lee, V. M. (2001) *J. Biol. Chem.* **276,** 2380–2386.
6. Weinreb, P. H., Zhen, W., Poon, A. W., Conway, K. A. & Lansbury, P. T., Jr. (1996) *Biochemistry* **35,** 13709–13715.
7. Eliezer, D., Kutluay, E., Bussell, R., Jr., & Browne, G. (2001) *J. Mol. Biol.* **307,** 1061–1073.
8. Hoyer, W., Cherny, D., Subramaniam, V. & Jovin, T. M. (2004) *Biochemistry* **43,** 16233–16242.
9. Bertoncini, C. W., Jung, Y. S., Fernandez, C. O., Hoyer, W., Griesinger, C., Jovin, T. M. & Zweckstetter, M. (2005) *Proc. Natl. Acad. Sci. USA* **102,** 1430–1435.
10. Chandra, S., Chen, X., Rizo, J., Jahn, R. & Sudhof, T. C. (2003) *J. Biol. Chem.* **278,** 15313–15318.
11. Jao, C. C., Der-Sarkissian, A., Chen, J. & Langen, R. (2004) *Proc. Natl. Acad. Sci. USA* **101,** 8331–8336.
12. Serpell, L. C., Berriman, J., Jakes, R., Goedert, M. & Crowther, R. A. (2000) *Proc. Natl. Acad. Sci. USA* **97,** 4897–4902.
13. Der-Sarkissian, A., Jao, C. C., Chen, J. & Langen, R. (2003) *J. Biol. Chem.* **278,** 37530–37535.
14. Fernandez, C. O., Hoyer, W., Zweckstetter, M., Jares-Erijman, E. A., Subramaniam, V., Griesinger, C. & Jovin, T. M. (2004) *EMBO J.* **23,** 2039–2046.
15. Uversky, V. N., Li, J. & Fink, A. L. (2001) *J. Biol. Chem.* **276,** 10737–10744.
16. Hoyer, W., Antony, T., Cherny, D., Heim, G., Jovin, T. M. & Subramaniam, V. (2002) *J. Mol. Biol.* **322,** 383–393.
17. Bernstein, S. L., Liu, D., Wyttenbach, T., Bowers, M. T., Lee, J. C., Gray, H. B. & Winkler, J. R. (2004) *J. Am. Soc. Mass Spectrom.* **15,** 1435–1443.
18. Munishkina, L. A., Phelan, C., Uversky, V. N. & Fink, A. L. (2003) *Biochemistry* **42,** 2720–2730.
19. Cohlberg, J. A., Li, J., Uversky, V. N. & Fink, A. L. (2002) *Biochemistry* **41,** 1502–1511.
20. Antony, T., Hoyer, W., Cherny, D., Heim, G., Jovin, T. M. & Subramaniam, V. (2003) *J. Biol. Chem.* **278,** 3235–3240.
21. Paik, S. R., Shin, H. J., Lee, J. H., Chang, C. S. & Kim, J. (1999) *Biochem. J.* **340,** 821–828.
22. Uversky, V. N., Li, J. & Fink, A. L. (2001) *J. Biol. Chem.* **276,** 44284–44296.
23. Yamin, G., Glaser, C. B., Uversky, V. N. & Fink, A. L. (2003) *J. Biol. Chem.* **278,** 27630–27635.
24. Bush, A. I. (2000) *Curr. Opin. Chem. Biol.* **4,** 184–191.
25. Sayre, L. M., Perry, G. & Smith, M. A. (1999) *Curr. Opin. Chem. Biol.* **3,** 220–225.
26. Lovell, M. A., Robertson, J. D., Teesdale, W. J., Campbell, J. L. & Markesbery, W. R. (1998) *J. Neurol. Sci.* **158,** 47–52.
27. Barnham, K. J., McKinstry, W. J., Multhaup, G., Galatis, D., Morton, C. J., Curtain, C. C., Williamson, N. A., White, A. R., Hinds, M. G., Norton, R. S., *et al.* (2003) *J. Biol. Chem.* **278,** 17401–17407.
28. Bush, A. I., Masters, C. L. & Tanzi, R. E. (2003) *Proc. Natl. Acad. Sci. USA* **100,** 11193–11194.
29. Atwood, C. S., Moir, R. D., Huang, X. D., Scarpa, R. C., Bacarra, N. M. E., Romano, D. M., Hartshorn, M. K., Tanzi, R. E. & Bush, A. I. (1998) *J. Biol. Chem.* **273,** 12817–12826.
30. Huang, X., Cuajungco, M. P., Atwood, C. S., Hartshorn, M. A., Tyndall, J. D., Hanson, G. R., Stokes, K. C., Leopold, M., Multhaup, G., Goldstein, L. E., *et al.* (1999) *J. Biol. Chem.* **274,** 37111–37116.
31. Brown, D. R. & Kozlowski, H. (2004) *J. Chem. Soc. Dalton Trans.* 1907–1917.
32. Viles, J. H., Cohen, F. E., Prusiner, S. B., Goodin, D. B., Wright, P. E. & Dyson, H. J. (1999) *Proc. Natl. Acad. Sci. USA* **96,** 2042–2047.
33. Aronoff-Spencer, E., Burns, C. S., Avdievich, N. I., Gerfen, G. J., Peisach, J., Antholine, W. E., Ball, H. L., Cohen, F. E., Prusiner, S. B. & Millhauser, G. L. (2000) *Biochemistry* **39,** 13760–13771.
34. Garnett, A. P. & Viles, J. H. (2003) *J. Biol. Chem.* **278,** 6795–6802.
35. Castellani, R. J., Siedlak, S. L., Perry, G. & Smith, M. A. (2000) *Acta Neuropathol.* **100,** 111–114.
36. Pall, H. S., Blake, D. R., Gutteridge, J. M., Williams, A. C., Lunec, J., Hall, M. & Taylor, A. (1987) *Lancet* **330,** 238–241.
37. Paik, S. R., Shin, H. J. & Lee, J. H. (2000) *Arch. Biochem. Biophys.* **378,** 269–277.
38. Hashimoto, M., Hsu, L. J., Xia, Y., Takeda, A., Sisk, A., Sundsmo, M. & Masliah, E. (1999) *NeuroReport* **10,** 717–721.
39. Miles, E. W. (1977) *Methods Enzymol.* **47,** 431–442.
40. Conway, K. A., Lee, S. J., Rochet, J. C., Ding, T. T., Williamson, R. E. & Lansbury, P. T., Jr. (2000) *Proc. Natl. Acad. Sci. USA* **97,** 571–576.
41. McCall, K. A. & Fierke, C. A. (2000) *Anal. Biochem.* **284,** 307–315.
42. Kuzmic, P. (1996) *Anal. Biochem.* **237,** 260–273.
43. Bryce, G. F. & Gurd, F. R. N. (1966) *J. Biol. Chem.* **241,** 122–129.
44. Daniele, P. G., Prenesti, E. & Ostacoli, G. (1996) *J. Chem. Soc. Dalton Trans.* 3269–3275.
45. Väängård, T. (1972) in *Biological Applications of Electron Spin Resonance*, eds. Swartz, H. M., Bolton, J. R. & Borg, D. C. (Wiley Interscience, New York), pp. 411–447.
46. Peisach, J. & Blumberg, W. E. (1974) *Arch. Biochem. Biophys.* **165,** 691–708.
47. Sakaguchi, U. & Addison, A. W. (1979) *J. Chem. Soc. Dalton Trans.* 600–608.
48. Lee, E. N., Lee, S. Y., Lee, D., Kim, J. & Paik, S. R. (2003) *J. Neurochem.* **84,** 1128–1142.
49. Bermel, W., Bertini, I., Felli, I. C., Kummerle, R. & Pierattelli, R. (2003) *J. Am. Chem. Soc.* **125,** 16423–16429.
50. Hartter, D. E. & Barnea, A. (1988) *J. Biol. Chem.* **263,** 799–805.
51. Hesse, L., Beher, D., Masters, C. L. & Multhaup, G. (1994) *FEBS Lett.* **349,** 109–116.
52. Garzon-Rodriguez, W., Yatsimirsky, A. K. & Glabe, C. G. (1999) *Bioorg. Med. Chem. Lett.* **9,** 2243–2248.
53. Karr, J. W., Jaupp, L. J. & Szalai, V. (2004) *J. Am. Chem. Soc.* **126,** 13534–13538.
54. Hornshaw, M. P., McDermott, J. R., Candy, J. M. & Lakey, J. H. (1995) *Biochem. Biophys. Res. Commun.* **214,** 993–999.
55. Brown, D. R., Qin, K., Herms, J. W., Madlung, A., Manson, J., Strome, R., Fraser, P. E., Kruck, T., von Bohlen, A., Schulz-Schaeffer, W., *et al.* (1997) *Nature* **390,** 684–687.